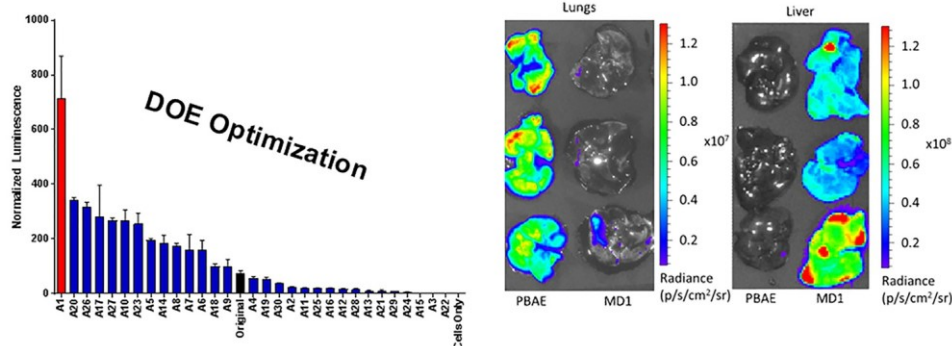


Optimization of a Degradable Polymer–Lipid Nanoparticle for Potent Systemic Delivery of mRNA to the Lung Endothelium and Immune Cells

James C. Kaczmarek,^{†,‡} Kevin J. Kauffman,^{†,‡} Owen S. Fenton,^{‡,§} Kaitlyn Sadtler,[‡] Asha Kumari Patel,^{†,||} Michael W. Heartlein,[‡] Frank DeRosa,[‡] and Daniel G. Anderson^{*,†,‡,§,||,N}

[†]Department of Chemical Engineering, [‡]David H. Koch Institute for Integrative Cancer Research, [§]Department of Chemistry, [#]Institute for Medical Engineering and Science, and ^NHarvard and MIT Division of Health Science and Technology, Massachusetts Institute of Technology, Cambridge, Massachusetts 02139, United States

^{||}Division of Cancer and Stem Cells, School of Medicine, University of Nottingham, Nottingham NG7 2RD, United Kingdom. [‡]Translate Bio, Lexington, Massachusetts 02421, United States



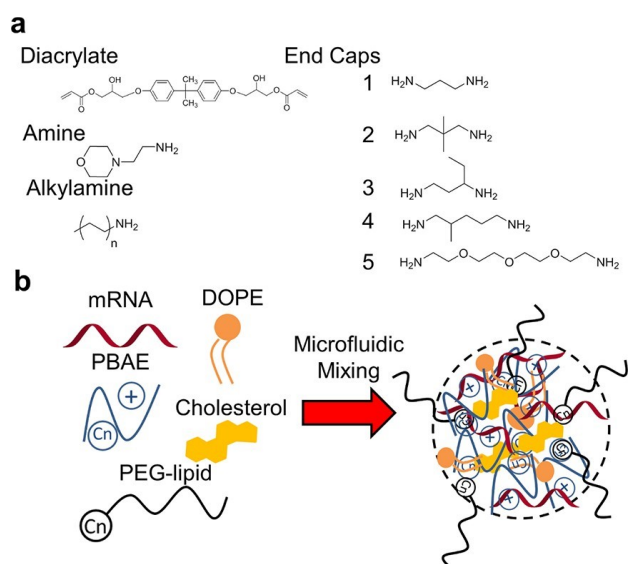
ABSTRACT: mRNA therapeutics hold great potential for treating a variety of diseases through protein-replacement, immunomodulation, and gene editing. However, much like siRNA therapy the majority of progress in mRNA delivery has been confined to the liver. Previously, we demonstrated that poly(β -amino esters), a class of degradable polymers, are capable of systemic mRNA delivery to the lungs in mice when formulated into nanoparticles with poly(ethylene glycol)–lipid conjugates. Using experimental design, a statistical approach to optimization that reduces experimental burden, we demonstrate herein that these degradable polymer–lipid nanoparticles can be optimized in terms of polymer synthesis and nanoparticle formulation to achieve a multiple order-of-magnitude increase in potency. Furthermore, using genetically engineered Cre reporter mice, we demonstrate that mRNA is functionally delivered to both the lung endothelium and pulmonary immune cells, expanding the potential utility of these nanoparticles.

KEYWORDS: mRNA Delivery, nanoparticles, polymers, optimization, PBAE

Recent advances in the synthesis of in vitro transcribed (IVT) mRNA have triggered an expansion of research into the delivery of such mRNAs for a variety of therapeutic purposes.¹ For the controlled production of specific proteins in vivo, delivery of mRNA is particularly attractive given its transient expression and elimination of risk for genomic insertion compared to DNA.² Therapeutic mRNA delivery requires bypassing a number of barriers, including RNase-mediated degradation, cellular entry, and endosomal escape.³ Considerable effort has been dedicated to the development of vectors that can transport nucleic acids to target cells in vivo.^{4,5} Nonviral nanoparticles, in particular, have emerged as promising mRNA delivery vehicles for a variety of applications including immunotherapy,^{6–9} protein replacement,^{10–12} and gene editing.^{13,14} However, like siRNA, the majority of work has focused on delivery to the liver following systemic delivery.^{4,5,11,15–17} Thus, the broadest realization of RNA therapeutics in the clinic requires the development of delivery vehicles capable of potent, specific mRNA delivery to a range of tissues, and, in particular, nonliver organs. For mRNA delivery, the lungs are a particularly interesting target, given the breadth of disease targets affecting endothelial,^{18,19} epithelial,^{20,21} and immune^{22,23} pulmonary cells. Schrom et al. recently reported the delivery of angiotensin-converting enzyme 2 mRNA to pulmonary cells following systemic delivery; however, their precise nanoparticle formulation was not disclosed.¹⁰

Previously, degradable poly(β -amino ester) (PBAE) nanoparticles formulated with poly(ethylene glycol)–(PEG–lipid) were developed and shown to facilitate delivery of mRNA selectively to the lung following systemic administration.²⁴ Here, we describe the improvement of this system using a design of experiment approach that uses statistical methods to limit necessary experimental conditions.¹⁷ We report a multiple order-of-magnitude increase in potency of mRNA delivery in vivo, while maintaining lung specificity.

A key feature of PBAE synthesis is its relative simplicity.^{25–27} The reaction proceeds through the Michael addition of an amine to a diacrylate under mild conditions with high conversion.²⁸ PBAE terpolymers incorporate an additional alkylamine in the backbone (see Supporting Information for reaction scheme).²⁹ Previous studies seeking to optimize PBAE nanoparticles have focused on the synthesis of libraries using a diverse set of monomers^{25,30} and altering polymer end-capping,³¹ molecular weight,³² and alkylamine chain length (in the case of terpolymers).²⁹ We sought to investigate the simultaneous evaluation of such synthesis parameters in the context of a single diacrylate/amine pair. Specifically, we chose to vary the end-capping group, the length of the alkylamine carbon chain, the molar ratio of diacrylate to amines (alters the molecular weight³³), and the molar ratio of the alkylamine to 4-(2-amino methyl) morpholine (Supporting Information Table S1). The diacrylate and amine chosen for this purpose, bisphenol A glycerolate and 4-(2-amino methyl) morpholine, respectively (Figure 1a), were identified as efficacious in previous studies of



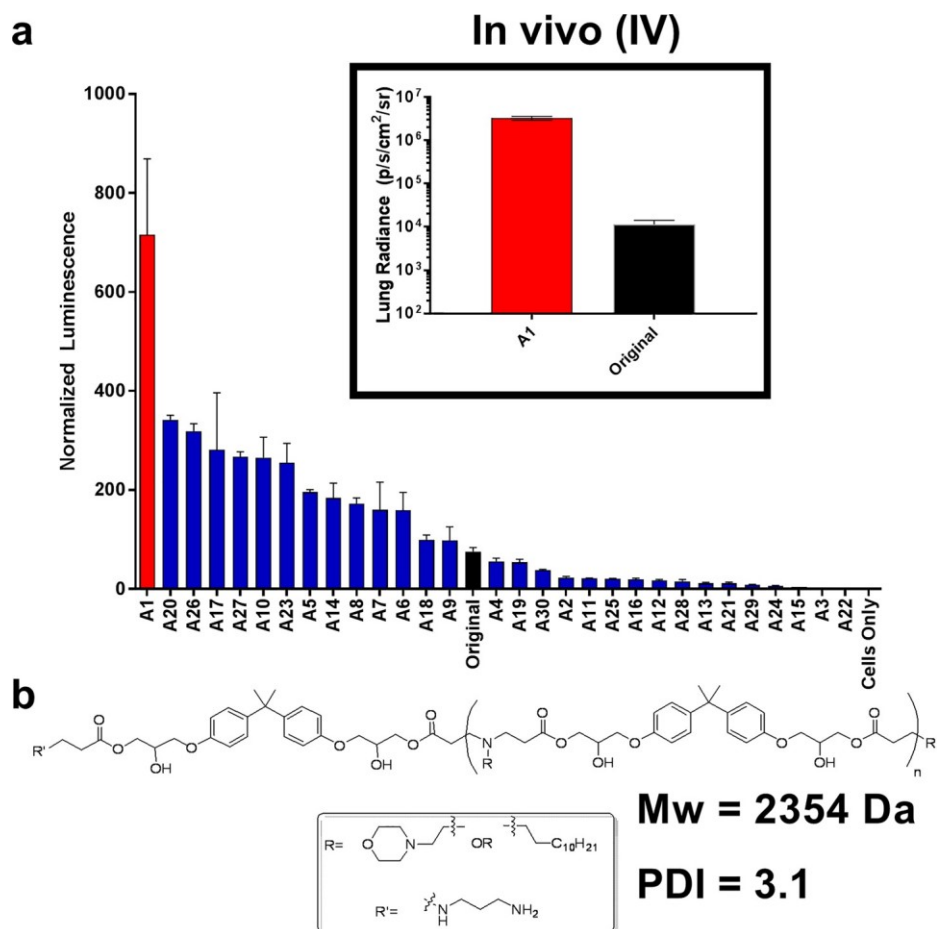


Figure 2. (a) A partial factorial screen optimizing PBAE synthesis parameters reveals several polymers more potent than the original when delivered in vitro in HeLa cells ($n = 4$). (insert) The top-performing polymer, A1 (red), is 2 orders of magnitude more potent in vivo in mouse lungs after IV delivery than the original, corresponding well to the in vitro results ($n = 3$). All particles were synthesized with luciferase-coding mRNA at an N/P of 57 with 7 wt % C14-PEG2000 PEG-lipid.²⁴ Note: 10^2 used as the minimum in the insert to account for magnitude of background luminescence. (b) Structural identity of A1 polymer.

In addition to optimizing the polymer synthesis, we sought to optimize the nanoparticle formulation, which has been shown to have a significant effect on mRNA delivery.¹⁷ Because the effects of formulation, such as changes in serum stability or biodistribution,²⁴ are not always identifiable in vitro, formulation screens were performed in vivo. The improvements in delivery through noncovalent formulation of PBAE terpolymers with PEG-lipid^{24,29} suggest that incorporation of other hydrophobic moieties may also improve function. As such, we sought to adapt lipid nanoparticle formulation strategies for use with PBAE materials. In particular, we sought to investigate the utility of 1,2-dioleoyl-*sn*-glycero-3-phosphoethanolamine (DOPE) and cholesterol when coformulated with PBAE polymers.¹⁷ In addition, we altered polymer N/P ratio, the PEG MW in the PEG-lipid, the phospholipid length in the PEG-lipid, and the molar composition of PEG-lipid in the formulation (Figure 1b).

Given that formulation with these moieties in the context of a PBAE terpolymer nanoparticle had not been reported, the potential design space was exceptionally broad. As such, we utilized a definitive screen, a special three-level screening design useful in narrowing a design space.³⁸ The parameter ranges chosen can be found in Supporting Information Table S3. Additionally, to ensure proper mixing of all

components, these particles were formulated using a microfluidic device that has been shown to consistently synthesize lipid nanoparticles with similar components.³⁹ As with the in vitro screen, we chose to use luciferase-coding mRNA as a reporter, as it would give us a means of quantifying protein production via image analysis while allowing us to visualize the biodistribution of mRNA translation. Synthesized particles were injected intravenously in female C57BL/6 mice (0.5 mg mRNA/kg mouse), and the mouse organs were excised and imaged for luminescence using an IVIS imaging apparatus 24 h following injection (Supporting Information Figure S12). As a control, deemed the “base formulation”, A1 polymer was formulated with only mRNA and 7 mol % C14-PEG2000 at the same ratios as used with the nonoptimized polymer (“original” polymer in Figure 2) in previous studies.²⁴ Figure 3a shows the results of this screen in the lungs and spleen, the two organs where luminescence was most prominent in the control particle (Supporting Information Figure S12). Only one formulation (D2) was more potent than the base formulation, and only one parameter, DOPE mol %, was statistically significant (Supporting Information Figure S3). However, the goal of the definitive screen was mainly to exclude less important variables.¹⁷

We based a subsequent partial factorial screen on a combination of the statistical model obtained from the screen as well as the parameters used in the D2 formulation

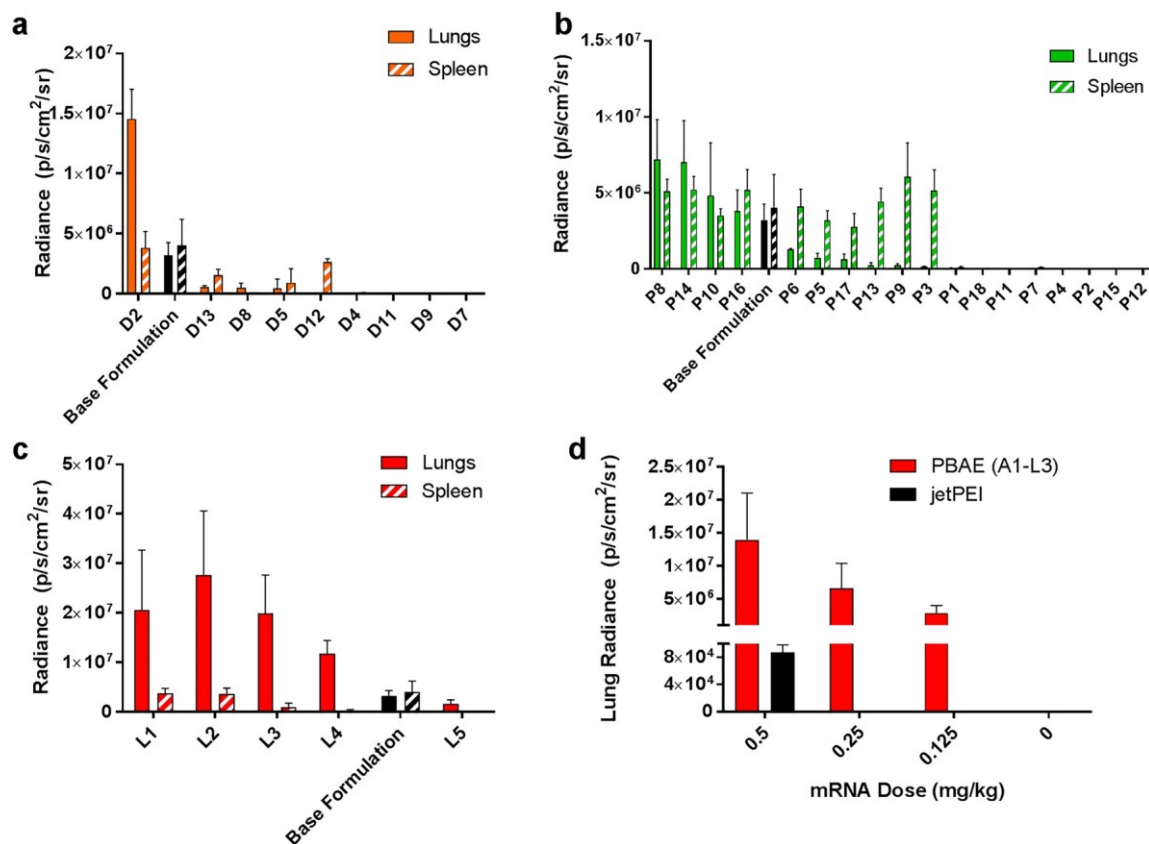


Figure 3. Luciferase-encoding mRNA was delivered via A1 PBAE nanoparticles intravenously in mice, and luminescence in various organs was assessed at 24 h. (a) A definitive screen revealed one formulation that was more potent than the base formulation (i.e., A1 polymer with 7 mol % C14-PEG2000 PEG-lipid). This formulation, along with statistical data from the screen, was used to develop the parameter space for a subsequent partial factorial screen. (b) The partial factorial screen had a greater number of formulations more potent in the lung (22% vs 7%), but several formulations showed high luciferase signal in the spleen. (c) By optimizing the mol % of PEG-lipid in the formulation, high lung-specificity could be obtained. (d) The optimized PBAE polymer/formulation (A1-L3) is orders of magnitude more potent than jetPEI across multiple mRNA doses ($n = 3$ for all experiments).

(Figure 3a, Supporting Information Table S3). Specifically, cholesterol and PEG-lipid chain length were eliminated and the remaining parameters were narrowed or altered in range. The parameters for this screen can be seen in Supporting Information Table S5, and a more detailed discussion of how these new parameters were chosen can also be found in the Supporting Information. Figure 3b shows that, as one would expect from successive screening, multiple formulations were more potent in the lungs than the base formulation. However, the partial factorial screen revealed several formulations that also transfected the spleen, and the overall lung-specificity of even those particles most effective in the lungs was decreased. To better understand the relationship between formulation and organ-specificity, we looked to the effects of PEG-lipid incorporation, which had a significant effect on both lung and spleen efficacy (Supporting Information Figures S4, S5). Another dependent variable, particle diameter, was also strongly correlated with PEG-lipid incorporation (Supporting Information Figure S6), so we investigated the relationship between particle size and efficacy. As can be seen in Supporting Information Figure S7, the nanoparticle formulations can be grouped into two distinct size regions: very small diameter (<100 nm), which corresponded to low efficacy, and large (>300 nm) diameter, which corresponded with high efficacy in both lung and spleen, with the spleen showing particularly consistent efficacy. Previous studies have

reported that larger particles tend to be endocytosed by splenocytes.⁴⁰ As for small-diameter particles, the two primary parameters exerting significant negative correlation on particle size were PEG MW and PEG-lipid mol %. This, too, is consistent with our data demonstrating that too much PEG-shielding of PBAE nanoparticles ablates their efficacy.²⁴ We therefore hypothesized that further optimization of PEG-lipid mol % could increase nanoparticle specificity for the lungs. We chose to manipulate PEG-lipid mol %, as it can be altered with higher precision than can the PEG MW, which is limited by the available molecular weights sold commercially. For this final PEG-lipid content-based screen, we synthesized nanoparticles with an N/P of 50, 20 mol % DOPE, and 1–7 mol % C18-PEG2000. All particles synthesized in this range, which yielded particle diameters within the region of interest (Supporting Information Figure S8), showed improved lung specificity (Figure 3c). Although formulation L2 (1.5 mol % PEG-lipid) showed the highest efficacy, we chose L3 (5 mol % PEG-lipid) as our optimized, lung-targeting formulation. L3 was not significantly less effective than L2, but it was almost half the size, which our data correlates with generally decreased weight loss following intravenous injection in mice (Supporting Information Figure S10). Overall, this optimized particle (referred to hereafter as A1-L3) was multiple orders of magnitude more effective than the commercially available in vivo jetPEI reagent across multiple doses (Figure 3d) and did not significantly alter

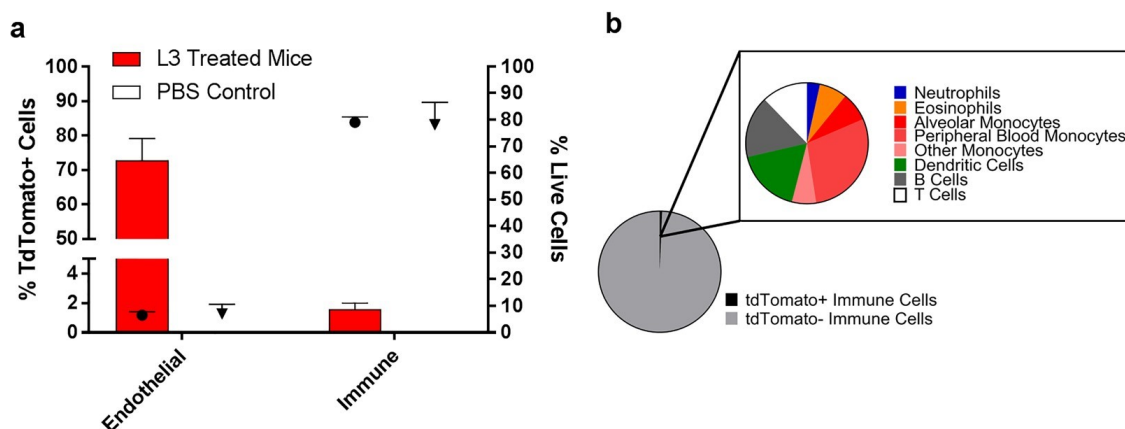


Figure 4. Analysis of lung cell types transfected using Ai14 Cre/lox reporter mice. (a) Percentages of cell types that were TdTomato+ (bars, left axis), indicating successful transfection with Cre mRNA using A1-L3 nanoparticles. Symbols (● for treated mice, ▼ for control mice, right axis) represent percentages of live cells which were either endothelial or immune cells ($n = 3$). (b) Identification of immune cell (CD45+) subtypes which express tdTomato following delivery of Cre mRNA via A1-L3 nanoparticles in Ai14 mice ($n = 2$).

liver enzyme levels at an intermediate dose (Supporting Information Figure S11). This particle also demonstrated a high degree of lung specificity compared to MD1 (also known as cKK-E12) lipid nanoparticles (Supporting Information Figure S13).^{16,41}

In general, the correlation between nanoparticle size and efficacy is tenuous at best,⁴² especially when one considers that the particle size measured in solution may not be the same in the context of plasma. Thus, we do not expect that this relationship will be fully translatable to all other mRNA delivery platforms. Nevertheless, for these specific nanoparticles we identified a correlation between size and lung-specificity (Supporting Information Figures S6–8, Figure 3c).

Having identified an optimized, lung-targeting particle, we sought to determine the cell populations within the lungs that were being transfected by this formulation. We utilized a mouse line expressing a tdTomato fluorophore cassette containing an upstream Lox-P flanked stop codon. After administering and expressing Cre-recombinase mRNA, this stop codon can be removed from the cassette, causing the cells which successfully translate Cre to constitutively express tdTomato.⁴³ Using this method, it is possible to identify with single cell resolution those cells to which mRNA is delivered.

A1-L3 nanoparticles were formulated with Cre-encoding mRNA, and delivered intravenously. Forty-eight hours later, the mouse lungs were harvested and processed into a single-cell suspension and analyzed using multicolor flow cytometry analysis. This formulation primarily transfected the lung endothelium with ~75% of endothelial cells expressing tdTomato (Figure 4a). The number of immune cells transfected (~2%) was low by comparison (Figure 4a).⁴⁴ As shown in Figure 4b, the majority of immune cells expressing protein are dendritic cells and various monocytes, although a portion of T and B cells were also transfected. (Supporting Information Figure S16).

In conclusion, we utilized a design of experiments to optimize a degradable, polymeric nanoparticle both in terms of polymer synthesis as well as nanoparticle formulation. This methodology allowed us to develop a polymer formulation two orders-of-magnitude more effective than its preoptimized form in vitro and in vivo

(Figure 2), and the use of successive formulation screens sequentially increased the efficacy of our nanoparticles while additionally allowing us to identify formulations that maintain lung-specificity (Figure 3). The utility of these designs of experiment methods in the context of a polymeric nanoparticle rather than a lipid nanoparticle further demonstrates its potential for in vivo optimization of RNA delivery vehicles.¹⁷ We envision that the use of experimental design in vivo may also be used to optimize nanoparticles for other organs as well. Moreover, the high level of mRNA expression in the lungs, coupled with these particles' ability to transfect pulmonary endothelial and immune cells (Figure 4) suggests that these particles may be useful in a variety of therapeutic contexts.

Experimental Section. Polymers were synthesized by dissolving diacrylate, amine, and alkyl amine monomers (concentration 1 M) in anhydrous *N,N*-dimethylformamide at various molar ratios for 48 h at 90 °C. End-capping monomer was then added at room temperature and reacted for an additional 24 h, followed by 2–3 washes with diethyl ether. Polymers were stored at –80 to –20 °C and dissolved in DMSO for formulation. Nanoparticles were synthesized by dissolving mRNA in sodium acetate buffer (pH 5.2) and polymer/hydrophobic moieties in ethanol as a separate phase. The two phases were mixed either by hand at a 1:1 v/v ratio or by microfluidic device at a 3:1 aqueous: ethanol v/v ratio. Statistical design and analysis was done using JMP software.

All animal experiments were approved by the MIT Institutional Animal Care and Use Committee and were consistent with local, state, and federal regulations as applicable.

SUPPORTING INFORMATION

The Supporting Information is available free of charge on the ACS Publications website at DOI: 10.1021/acs.nanolett.8b02917.

Chemical synthesis and characterization; extended experimental methods; experimental design methodology; additional data; additional figures, tables, and works cited (PDF)

Notes

The authors declare the following competing financial interest(s): MWH and FD are employees of Translate Bio.

ACKNOWLEDGMENTS

The authors would like to acknowledge project funding by Translate Bio (Lexington, MA) in addition to partial funding from the Cancer Center Support (core) Grant P30-CA14051 from the NCI. The authors acknowledge the contribution of the Koch Institute Nanotechnology Materials Core, Animal Imaging and Preclinical Testing Core, and Flow Cytometry Core.

REFERENCES

- (1) Kaczmarek, J. C.; Kowalski, P. S.; Anderson, D. G. *Genome Med.* 2017, *9*, 60.
- (2) Yamamoto, A.; Kormann, M.; Rosenecker, J.; Rudolph, C. *Eur. J. Pharm. Biopharm.* 2009, *71* (3), 484–489.
- (3) Dowdy, S. F. *Nat. Biotechnol.* 2017, *35* (3), 222–229.
- (4) Kauffman, K. J.; Webber, M. J.; Anderson, D. G. *J. Controlled Release* 2016, *240*, 227–234.
- (5) Guan, S.; Rosenecker, J. *Gene Ther.* 2017, *24* (3), 133–143.
- (6) Pardi, N.; Secreto, A. J.; Shan, X.; Debonera, F.; Glover, J.; Yi, Y.; Muramatsu, H.; Ni, H.; Mui, B. L.; Tam, Y. K.; et al. *Nat. Commun.* 2017, *8*, 14630.
- (7) Stadler, C. R.; Bañ-Mahmud, H.; Celik, L.; Hebich, B.; Roth, A. S.; Roth, R. P.; Karikó, K.; Türeci, O.; Sahin, U. *Nat. Med.* 2017, *23*, 1241.
- (8) Su, X.; Fricke, J.; Kavanagh, D. G.; Irvine, D. J. *Mol. Pharmaceutics* 2011, *8* (3), 774–787.
- (9) Chahal, J. S.; Khan, O. F.; Cooper, C. L.; McPartlan, J. S.; Tsosie, J. K.; Tilley, L. D.; Sidik, S. M.; Lourido, S.; Langer, R.; Bavari, S.; et al. *Proc. Natl. Acad. Sci. U. S. A.* 2016, *113* (29), E4133–E4142.
- (10) Schrom, E.; Huber, M.; Aneja, M.; Dohmen, C.; Emrich, D.; Geiger, J.; Hasenpusch, G.; Herrmann-Janson, A.; Kretzschmann, V.; Mykhailik, O.; et al. *Mol. Ther.–Nucleic Acids* 2017, *7* (June), 350–365.
- (11) DeRosa, F.; Guild, B.; Karve, S.; Smith, L.; Love, K.; Dorkin, J. R.; Kauffman, K. J.; Zhang, J.; Yahalom, B.; Anderson, D. G.; et al. *Gene Ther.* 2016, *23* (10), 699–707.
- (12) Mahiny, A. J.; Dewerth, A.; Mays, L. E.; Alkhaled, M.; Mothes, B.; Malaeksefat, E.; Loretz, B.; Rottenberger, J.; Brosch, D. M.; Reautschnig, P.; et al. *Nat. Biotechnol.* 2015, *33* (6), 584–586.
- (13) Yin, H.; Song, C.-Q.; Dorkin, J. R.; Zhu, L. J.; Li, Y.; Wu, Q.; Park, A.; Yang, J.; Suresh, S.; Bizhanova, A.; et al. *Nat. Biotechnol.* 2016, *34* (3), 328–333.
- (14) Miller, J. B.; Zhang, S.; Kos, P.; Xiong, H.; Zhou, K.; Perelman, S. S.; Zhu, H.; Siegwart, D. J. *Angew. Chem., Int. Ed.* 2017, *56* (4), 1059–1063.
- (15) Kanasty, R.; Dorkin, J. R.; Vegas, A.; Anderson, D. *Nat. Mater.* 2013, *12* (11), 967–977.
- (16) Fenton, O. S.; Kauffman, K. J.; McClellan, R. L.; Appel, E. A.; Dorkin, J. R.; Tibbitt, M. W.; Heartlein, M. W.; DeRosa, F.; Langer, R.; Anderson, D. G. *Adv. Mater.* 2016, *28* (15), 2939–2943.
- (17) Kauffman, K. J.; Dorkin, J. R.; Yang, J. H.; Heartlein, M. W.; DeRosa, F.; Mir, F. F.; Fenton, O. S.; Anderson, D. G. *Nano Lett.* 2015, *15* (11), 7300–7306.
- (18) Green, C. E.; Turner, A. M. *Respir. Res.* 2017, *18* (1), 20.
- (19) Leus, N. G. J.; Morselt, H. W. M.; Zwieters, P. J.; Kowalski, P. S.; Ruiters, M. H. J.; Molema, G.; Kamps, J. A. A. M. *Int. J. Pharm.* 2014, *469* (1), 121–131.
- (20) Bals, R.; Hiemstra, P. S. *Eur. Respir. J.* 2004, *23* (2), 327–333.
- (21) Griesenbach, U.; Alton, E. W. F. W. *Hum. Mol. Genet.* 2013, *22*

(R1), R52–8.

(22) Kim, E. Y.; Battaile, J. T.; Patel, A. C.; You, Y.; Agapov, E.; Grayson, H.; Benoit, L. A.; Byers, D. E.; Alevy, Y.; Tucker, J.; et al. *Nat. Med.* 2008, *14* (6), 633–640.

(23) Grumelli, S.; Corry, D. B.; Song, L.; Song, L.; Green, L.; Huh, J.; Hacken, J.; Espada, R.; Bag, R.; Lewis, D. E.; et al. *PLoS Med.* 2004, *1* (1), e8.

(24) Kaczmarek, J. C.; Patel, A. K.; Kauffman, K. J.; Fenton, O. S.; Webber, M. J.; Heartlein, M. W.; DeRosa, F.; Anderson, D. G. *Angew. Chem., Int. Ed.* 2016, *55* (44), 13808–13812.

(25) Anderson, D. G.; Lynn, D. M.; Langer, R. *Angew. Chem., Int. Ed.* 2003, *42* (27), 3153–3158.

(26) Cutlar, L.; Zhou, D.; Gao, Y.; Zhao, T.; Greiser, U.; Wang, W.; Wang, W. *Biomacromolecules* 2015, *16* (9), 2609–2617.

(27) Gao, Y.; Huang, J.; O’Keeffe Ahern, J.; Cutlar, L.; Zhou, D.; Lin, F.-H.; Wang, W. *Biomacromolecules* 2016, *17* (11), 3640–3647.

(28) Lynn, D. M.; Langer, R. *J. Am. Chem. Soc.* 2000, *122* (44), 10761–10768.

(29) Eltoukhy, A. a.; Chen, D.; Alabi, C. a.; Langer, R.; Anderson, D. G. *Adv. Mater.* 2013, *25*, 1487–1493.

(30) Shmueli, R. B.; Sunshine, J. C.; Xu, Z.; Duh, E. J.; Green, J. J. *Nanomedicine* 2012, *8* (7), 1200–1207.

(31) Zugates, G. T.; Peng, W.; Zumbuehl, A.; Jhunjunwala, S.; Huang, Y.-H.; Langer, R.; Sawicki, J. a.; Anderson, D. G. *Mol. Ther.* 2007, *15* (7), 1306–1312.

(32) Eltoukhy, A. a.; Siegwart, D. J.; Alabi, C. a.; Rajan, J. S.; Langer, R.; Anderson, D. G. *Biomaterials* 2012, *33*, 3594–3603.

(33) Odian, G. *Fourth*; John Wiley & Sons, Inc.: Hoboken, NJ, 2004.

(34) Jarzębńska, A.; Pasewald, T.; Lambrecht, J.; Mykhaylyk, O.; Kümmerling, L.; Beck, P.; Hasenpusch, G.; Rudolph, C.; Plank, C.; Dohmen, C. *Angew. Chem., Int. Ed.* 2016, *55* (33), 9591–9595.

(35) Sunshine, J. C.; Akanda, M. I.; Li, D.; Kozielski, K. L.; Green, J. J. *Biomacromolecules* 2011, *12* (10), 3592–3600.

(36) Sahay, G.; Querbes, W.; Alabi, C.; Eltoukhy, A.; Sarkar, S.; Zurenko, C.; Karagiannis, E.; Love, K.; Chen, D.; Zoncu, R.; et al. *Nat. Biotechnol.* 2013, *31* (7), 653–658.

(37) Gilleron, J.; Querbes, W.; Zeigerer, A.; Borodovsky, A.; Marsico, G.; Schubert, U.; Manygoats, K.; Seifert, S.; Andree, C.; Stoeter, M.; et al. *Nat. Biotechnol.* 2013, *31* (June), 638–646.

(38) Jones, B.; Nachtsheim, C. J. *J. Qual. Technol.* 2011, *43* (1), 1–15.

(39) Chen, D.; Love, K. T.; Chen, Y.; Eltoukhy, A. A.; Kastrup, C.; Sahay, G.; Jeon, A.; Dong, Y.; Whitehead, K. A.; Anderson, D. G. *J. Am. Chem. Soc.* 2012, *134* (16), 6948–6951.

(40) Blanco, E.; Shen, H.; Ferrari, M. *Nat. Biotechnol.* 2015, *33* (9), 941–951.

(41) Dong, Y.; Love, K. T.; Dorkin, J. R.; Sirirungruang, S.; Zhang, Y.; Chen, D.; Bogorad, R. L.; Yin, H.; Vegas, A. J.; Alabi, C. A.; et al. *Proc. Natl. Acad. Sci. U. S. A.* 2014, *111* (11), 3955.

(42) Whitehead, K. a.; Matthews, J.; Chang, P. H.; Niroui, F.; Dorkin, J. R.; Severgnini, M.; Anderson, D. G. *ACS Nano* 2012, *6*, 6922–6929.

(43) Kauffman, K. J.; Oberli, M. A.; Dorkin, J. R.; Hurtado, J. E.; Kaczmarek, J. C.; Bhadini, S.; Wyckoff, J.; Langer, R.; Jaklenc, A.; Anderson, D. G. *Mol. Ther.–Nucleic Acids* 2018, *10* (March), 55–63.

(44) Bantikasegn, A.; Song, X.; Politi, K. *Am. J. Respir. Cell Mol. Biol.* 2015, *52* (4), 409–417.